Acta Crystallographica Section B
Structural Science
ISSN 0108-7681

Charge density distribution in aminomethylphosphonic acid

Rafał Janicki and Przemysław Starynowicz*

Wydział Chemii, Uniwersytet Wrocławski, ul. F. Joliot-Curie 14, 50-383 Wrocław, Poland

Correspondence e-mail: psta@wchuwr.pl

Received 8 February 2010
Accepted 1 July 2010

The experimental charge density distribution in aminomethylphosphonic acid has been determined from X-ray diffraction and its topological features have been analyzed. The results have shown that the P—O bonds are highly polarized, moreover the P—OH bond is weaker than the bonds to unprotonated O atoms. These facts have been confirmed by theoretical density functional theory (DFT) calculations, which have shown that the single, strongly polarized bonds within the phosphonate group are modified by hyperconjugation effects.

1. Introduction

Phosphorus is one of the crucial elements in the chemistry of life (Westheimer, 1987), being a component of nucleic acids, as a variety of organic phosphates, enzymes and intermediates in metabolic pathways (Savigniac & Iorga, 2003; Murphy, 2004). Various phosphonates, in turn, have been widely applied, *e.g.* in medical diagnostics (Winter *et al.*, 1998), therapy (Gasiglia & Okada, 1995; Finlay *et al.*, 2005; Schwartz, 2006) and agriculture. The importance of these compounds has prompted extensive experimental and theoretical investigations. Phosphorus has an electronic structure of the valence shell which is analogous to nitrogen, but the two elements have different properties and create different compounds. The phosphate and phosphonate groups form distorted tetrahedra in which the central atom is in the formal oxidation state +3 or +5. Such structures apparently break the octet rule, as for compatibility with the P and O valence an additional fifth bond originating from the P atom is required to present the Lewis structures of these compounds in covalent form. Apart from this the P—O bonds are generally shorter than expected (Schomaker & Stevenson, 1941). These difficulties have raised the question about the nature of the bonds formed by phosphorus. Preliminary ideas about the involvement of the *d* orbitals of phosphorus (Mitchell, 1969) were refuted on the basis of further extensive computational studies (Magnusson, 1990), which have demonstrated that the empty *d* orbitals have too much energy to form effective hybrids with the *s* and *p* orbitals. The excitation energy of $3s \rightarrow 3d$ is *ca* 16.5 eV (Hudson, 1964), therefore an explanation had to be sought within the *s* and *p* orbitals only. Different approaches have been put forward: a three-centre, four electron-bond system, negative hyperconjugation or the formation of bent Ω (banana) bonds (Gilheany, 1994; Denehy *et al.*, 2007).

It is useful to confront the computational results with those obtained from an empirical electron density distribution. Such a distribution may be obtained by X-ray diffraction. Although caution must be taken when comparing properties and quantities derived from experiment and calculated theoreti-

Table 1
Experimental details.

Crystal data	
Chemical formula	CH_6NO_3P
M_r	111.04
Crystal system, space group	Orthorhombic, *Pbca*
Temperature (K)	85
a, *b*, *c* (Å)	8.977 (7), 9.186 (7), 10.003 (7)
V (Å^3)	824.9 (11)
Z	8
Radiation type	Mo *Kα*
μ (mm^{-1})	0.53
Crystal size (mm)	0.38 × 0.30 × 0.21
Data collection	
Diffractometer	Goniometer Xcalibur, detector: Onyx
Absorption correction	Analytical
T_{min}, T_{max}	0.886, 0.942
No. of measured, independent and observed [$I > 2\sigma(I)$] reflections	80 581, 8632, 6898
R_{int}	0.041
Conventional refinement	
Refinement method	Full-matrix least-squares on F^2
Data/restraints/parameters	8630/0/79
Goodness-of-fit on F^2	2.000
Final *R* indices [$I > 2\sigma(I)$]	$R(F) = 0.0217$, $wR(F^2) = 0.0452$
R indices (all data)	$R(F) = 0.0308$, $wR(F^2) = 0.0463$
$\Delta\rho_{max}$, $\Delta\rho_{min}$ (e Å^{-3})	0.515, −0.705
Refinement (I)	
Refinement method	Full-matrix least-squares on *F*
Data/restraints/parameters	4737/0/224
Goodness-of-fit on *F*	1.357
Final *R* indices [$F > 3\sigma(F)$]	$R(F) = 0.0128$, $wR(F^2) = 0.0241$
$\Delta\rho_{max}$, $\Delta\rho_{min}$ (e Å^{-3})	0.314, −0.273
Refinement (II)	
Refinement method	Full-matrix least-squares on *F*
Data/restraints/parameters	4737/0/219
Goodness-of-fit on *F*	1.338
Final *R* indices [$F > 3\sigma(F)$]	$R(F) = 0.0127$, $wR(F^2) = 0.0238$
$\Delta\rho_{max}$, $\Delta\rho_{min}$ (e Å^{-3})	0.289, −0.224

Computer programs: *CrysAlisPro* (Oxford Diffraction Ltd, 2010), *SHELXS*97, *SHELXL*97 (Sheldrick, 2008).

cally (the former represents a molecule surrounded by its interacting neighbors, whereas the theoretical approach often deals with the molecule *in vacuo*), useful conclusions may be reached. As far as the phosphonates or phosphates are concerned, there has been only a limited number of experimental studies of charge density distributions. The systems that have been investigated include, among others, hydrogen [(2,4-diamino-pyrimidin-1-io)methyl]phosphonate monohydrate (hereinafter abbreviated as HPPM; Slouf *et al.*, 2002), diphenylphosphonic acid (Lyssenko *et al.*, 2002), phosphoric acid (Souhassou *et al.*, 1995), ammonium dihydrogen phosphate (Pérès *et al.*, 1999), L-arginine dihydrogen phosphate (Espinosa *et al.*, 1996), sodium dihydrogen phosphate (Ichikawa *et al.*, 1998), $AlPO_4$-15 molecular sieve (Aubert *et al.*, 2003) and urea–phosphoric acid (1/1) (Rodrigues *et al.*, 2001). The absence of simple phosphonates which might serve as model compounds for theoretical and experimental studies may be noted. On the other hand, great interest in aminophosphonic compounds, resulting from their potential use in medicine in the form of complexes with the *f* and *d* elements, has been recently observed (Mondry & Janicki, 2006; Mao, 2007; Janicki & Mondry, 2008). Moreover, lanthanide complexes with aminophosphonic ligands display interesting spectroscopic properties which may give rise to their application as luminescence probes (Parker, 2004). For these reasons we have decided to study the electron density distribution in a simple aminomethylphosphonic acid – $NH_2CH_2PO_3H_2$ – expecting that such an investigation may provide helpful information about the nature of the bonds within the phosphonate group.

The crystal structure of this compound has been described by Darriet *et al.* (1975). The compound crystallizes in the centrosymmetric group *Pbca*. The crystals are composed of small aminomethylphosphonic acid molecules, which are in the zwitterionic form. These factors rendered the compound ideal for experimental determination of the charge density distribution.

2. Experimental

2.1. Data collection and refinement

Crystals were grown from a water solution. A suitable crystal was cut from a larger one and mounted on an Xcalibur diffractometer equipped with a tube with a Mo anode, a graphite monochromator, an Onyx CCD detector and an Oxford Cryosystem device. Quick preliminary data collection and structure refinement showed that the crystal quality was good enough for the determination of the charge density distribution. The data up to $\sin(\theta/\lambda) = 1.366$ Å^{-1} were then collected at 85 K and the intensities were corrected for Lorentz, polarization and absorption factors, the latter calculated from the crystal habit. Apart from that, detector area scaling was applied using a 10 × 10 grid; the software used for the data reduction was *CrysAlis CCD* (Oxford Diffraction Ltd, 2010); 80 581 intensities were recorded. The data were then scaled and averaged with *SORTAV* (Blessing, 1987), 11 outliers were removed; R_{int} was 0.0208 for reflections up to $\sin(\theta/\lambda) = 0.7$ Å^{-1}, 0.0294 for $\sin(\theta/\lambda) \leq 1.15$ Å^{-1}, and 0.0306 for all data. The conventional refinement was performed with *SHELX*97 (Sheldrick, 2008) and all the H atoms were refined freely, see Table 1 for details.[1]

The multipole refinement was performed with *XD*2006 (Volkov *et al.*, 2006) in the following way. The data merged with *SORTAV*, together with the results of the conventional refinement, were transferred to *XD*. The multipole expansion formula for each atom was

$$\rho(\mathbf{r}) = \rho_c(\mathbf{r}) + P_v\rho_v(\kappa\mathbf{r}) + \sum_l R_l(\kappa' r)\sum_{m=-l}^{l} P_{lm}y_{lm}, \qquad (1)$$

where ρ is the charge distribution function, ρ_c and ρ_v represent the core and spherical valence, R_l is the radial function used for the aspherical deformation terms, P_v and P_{lm} are empirically fitted valence and multipole populations, y_{lm} are real

[1] Supplementary data for this paper are available from the IUCr electronic archives (Reference: SO5036). Services for accessing these data are described at the back of the journal.

spherical harmonics, and κ and κ' are screening parameters (Hansen & Coppens, 1978). The scattering factors calculated from Clementi–Roetti wavefunctions (Clementi & Roetti, 1974) for the core and spherical valence parts of the atomic charge distribution were used. The radial deformation functions $R_l(r)$ were in the form of single Slater functions $[\zeta^{n+3}/(n+2)!]r^n\exp(-\zeta r)$. For phosphorus the n value was set to 6, following Espinosa *et al.* (1996), and the initial ζ value, 5.19 bohr^{-1} for all l, was obtained by multiplying 3.46 bohr^{-1}, calculated from the relevant Clementi–Roetti radial functions for n = 4, by 1.5. The final $\kappa'\zeta$ values for all atom types are given in Table S6 of the supplementary material. Two multipole refinement versions were attempted. Both were against the observed structure factors F, with the C—H distances fixed at 1.09 Å, N—H at 1.03 Å and O—H at 0.96 Å (Allen *et al.*, 1987). The data with $F \geq 3\sigma(F)$ up to $\sin(\theta/\lambda)$ = 1.15 Å^{-1} were included in the calculations. The displacement vibration factors were harmonic anisotropic for the non-H atoms and isotropic for the H atoms. Isotropic extinction of type I (mosaic distribution dominated; Gaussian distribution) was refined with the absorption path length set as 0.3 mm (the mean of the crystal dimensions). The extinction was not severe, nevertheless, its inclusion allowed the improvement of the final parameters. The most affected reflection was 200 with a y (= $F^2_{\rm corr}/F^2_{\rm uncorr}$) value of 0.77, apart from that three others had y between 0.85 and 0.90 and five others had y between 0.90 and 0.95. The weighting scheme was $w = 1/\sigma^2(F)$.

In both refinement variants the C, N and O atoms were modelled as octupoles and the H atoms as quadrupoles; the κ parameters for non-H atoms were refined, whereas κ and κ' for H were kept fixed at 1.2. The modelling of H atoms as quadrupoles with isotropic displacement factors implies that the possible anisotropy of thermal vibrations is transferred to the quadrupole parameters and the static electron density around these atoms cannot be deconvoluted from the vibrations. We have nevertheless decided to adopt such an approach in order to avoid spurious absorption of unaccounted hydrogen displacement anisotropy by parameters of other atoms. Inclusion of quadrupolar terms for H atoms improved the charges of the P and O atoms, and limited expansion of the O atoms (*i.e.* a decrease in κ', when this parameter was refined), whereas it brought about only moderate changes around H atoms. In the first variant [labelled as refinement (I)] the calculations were performed with P-atom density expanded up to hexadecapoles, whereas all k' factors were kept fixed (κ' = 1.0 for non-H atoms). In the other refinement [variant (II)] phosphorus was modelled as an octupole. All κ' coefficients except those of H were freely refined. The refinement parameters for both variants are given in Table 1. The inclusion of extinction reduced $R(F)$ from 0.0142 to 0.0133 for refinement (I) and from 0.133 to 0.130 for (II), and brought about smoothing of the residual density maps. An attempt to include hexadecapoles in refinement (II) for P improved to some extent the residual maps and the refinement parameters, but led to poorer atom net charges (the P-atom charge was −0.5 and the O atoms were almost neutral), and therefore was abandoned. During both refinements no symmetry or chemical constraints were imposed on multipole expansion parameters.

The Hirshfeld test (Hirshfeld, 1976) showed that the differences between mean-square displacement amplitudes did not exceed 1.1 × 10^{-3} Å^2, the largest value being for the P—C bond.

2.2. Theoretical calculations

The DFT calculations were performed with the *ADF* suite of programs (Baerends *et al.*, 2008). In the first step the positions of the H atoms were optimized, whereas the positions of the non-H atoms were kept fixed as input from the X-ray conventional refinement. Also, the bond angles H—N—C and the torsion angles H—N—C—P were frozen, otherwise H4 tended to migrate towards O2. The functional used was PW91, and the basis TZ2P composed of double ζ functions for core electrons, triple ζ for valence ones and two polarization functions; the core was not frozen. The second step included calculations of the final wavefunctions of the molecule and their analysis. At this stage the calculations were performed with PW91 and two bases: TZ2P and ET-QZ3P-1DIFFUSE (even-tempered, 9*s* 7*p* 4*d* 2*f* for P, 7*s* 5*p* 3*d* 2*f* for C, N and O, 5*s* 3*p* 2*d* for H). The natural bond orbitals (NBO) analysis, together with the calculation of resonance Lewis structures, was performed with NBO 5.0 (Glendening *et al.*, 2001). As both calculations were generally in good agreement, only the results for the TZ2P basis will be discussed in detail. Wherever appropriate, the results obtained for the ET-QZ3P-1DIFFUSE basis will be marked with an ET label.

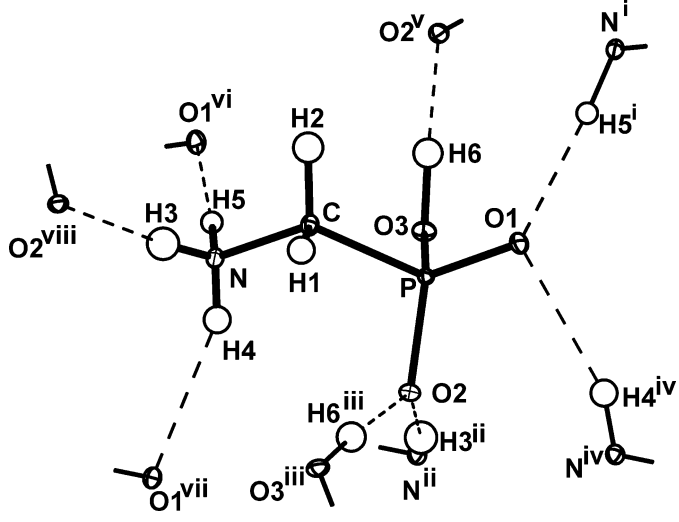

Figure 1
View of aminomethylphosphonic acid together with hydrogen bonds (dashed lines). The symmetry codes are the same as in Table 3 plus: (iv) $-\frac{1}{2}-x, 1-y, \frac{1}{2}+z$; (v) $-\frac{1}{2}-x, \frac{1}{2}+y, z$; (vi) $-x, \frac{3}{2}-y, -\frac{1}{2}+z$; (vii) $-\frac{1}{2}-x, 1-y, -\frac{1}{2}+z$; (viii) $-\frac{1}{2}+x, y, \frac{1}{2}-z$. The ellipses are drawn at 30% probability.

3. Results and discussion

A *DIAMOND*3.0 (Brandenburg & Putz, 2005) view of the molecule together with the hydrogen bonds that the molecule is involved in is presented in Fig. 1. The bond lengths and angles from the conventional refinement and those from the two multipole ones (see the CIF file for the values) do not differ significantly.

The residual maps from both multipole refinements (Fig. 2) are essentially featureless with values rarely exceeding 0.10 e Å^{-3}, the highest peaks and holes being around phosphorus. This may be connected to imperfect modeling of the density around this atom with Slater's single ζ functions (Souhassou *et al.*, 1995; Volkov & Coppens, 2001) and/or by the influence of residues of unaccounted absorption. (We have attempted various treatments of the absorption corrections and the region around phosphorus was the most affected on the residual density maps.)

The charges obtained from the multipole refinements, *i.e.* those derived from multipole populations, hereinafter named experimental, as well as Hirshfeld (1977) and Bader (1990) charges, together with those calculated theoretically (Hirshfeld and Bader charges) are presented in Table 2. Refinement (II) yields a smaller multipole charge for P, although that from (I) is also smaller than that in a published phosphonate (HPPM; Slouf *et al.*, 2002) – 0.62 – but it resembles the charge in H_3PO_4 (Souhassou *et al.*, 1995) – 0.42 (11). The non-protonated O atoms in our compound (O1 and O2) are more negatively charged than the hydroxyl O3, which is consistent with the behaviour reported in the quoted compounds. In the phosphonate mentioned above the unprotonated O atoms had the charges −0.66 (3) and −0.72 (3); −0.42 (3) for the protonated one; −0.47 (5) for the unprotonated O of the phosphoric acid; −0.17(4) for the protonated one. On the other hand, a fairly good correspondence may be observed between the theoretically and experimentally derived Hirshfeld and Bader pseudoatom charges. However, one may notice that refinement (I) yields more polarized values of the experimental charges for the phosphonate group than refinement (II). On the other hand, the Hirshfeld and Bader charges are more diverse for refinement (II). Both refinements underestimate the Hirshfeld charge of phosphorus in comparison to the theoretical DFT value. Apart from that the Bader charge of P from refinement (I) is *ca* 0.4 e smaller than those from refinement (II) and the DFT calculations. The Hirshfeld and Bader charges of O atoms from both refinements are comparable, although refinement (II) better illustrates the difference between the unprotonated oxygen atoms O1 or O2, and the protonated O3. The values of Bader charges obtained for the P and O atoms in the present compound from refinement (II) and the DFT calculations are in good agreement with those reported for $AlPO_4$-15 molecular sieves [P 3.45 and 3.48, O(phosphate) −1.43 and −1.53]. The Hirshfeld sum charges of the phosphonate $-PO_3H$ group are comparable, whereas the Bader one calculated *ab initio* is in better agreement with that obtained from refinement (II) than that from (I).

Essential topological parameters of the charge distribution for both refinements, together with calculated Wiberg (1968) bond orders, are summarized in Table 3 (see supplementary material for full tables). Comparison of ρ_c (the charge

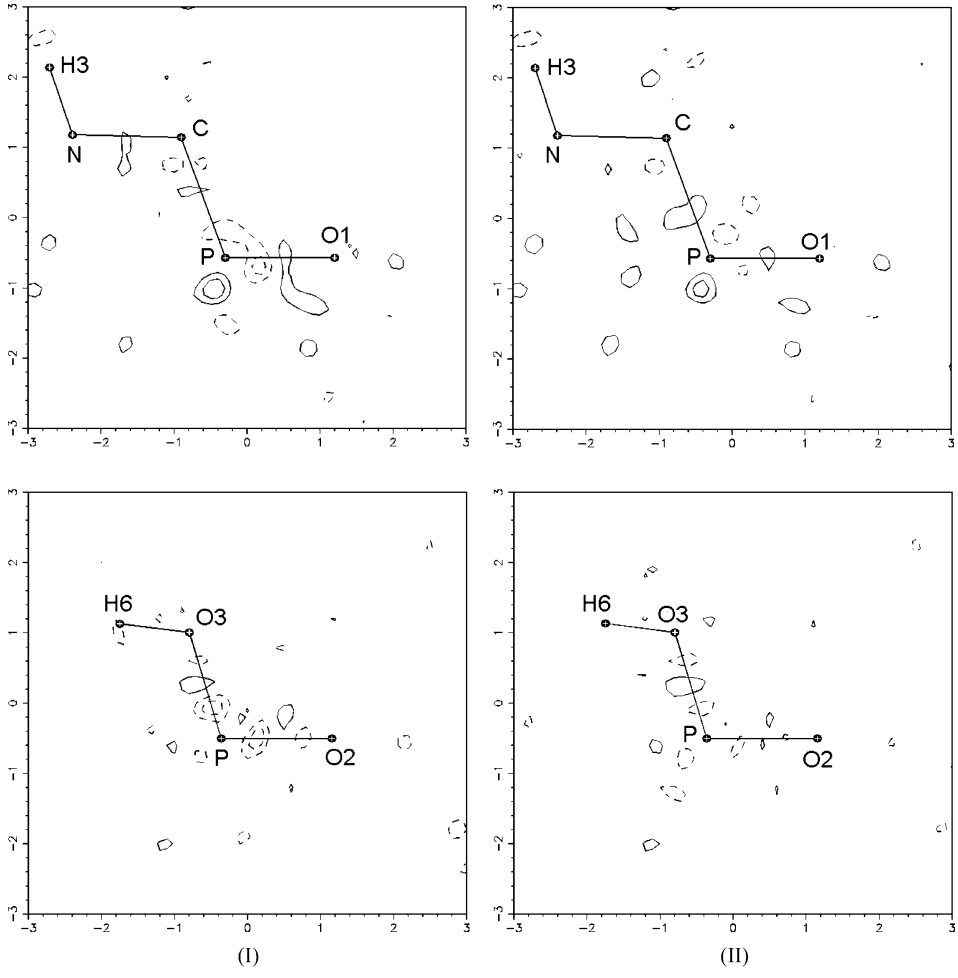

Figure 2
Residual density maps for multipole refinements (I) and (II). The contour intervals are drawn at 0.1 e Å^{-3}; the positive contours are solid, the negative contours are dashed and the zero contours have been omitted. The scale is shown in Å and the sections are through the (C,P,O1) and (O2,P,O3) planes.

Table 2
The atom charges obtained from multipole refinements and DFT calculations.

The charges are labelled as follows: Q_{mp}: from multipole populations, Q_B: Bader charges from integration over atomic basins and Q_H: Hirshfeld.

	Refinement (I)			Refinement (II)			DFT (TZ2P)	
Atom	Q_{mp}	Q_B	Q_H	Q_{mp}	Q_B	Q_H	Q_B	Q_H
P	0.45 (6)	3.02	0.16	0.02 (8)	3.41	0.19	3.44	0.32
O1	−0.50 (2)	−1.37	−0.41	−0.33 (3)	−1.52	−0.48	−1.45	−0.43
O2	−0.52 (2)	−1.32	−0.42	−0.38 (3)	−1.41	−0.45	−1.48	−0.43
O3	−0.41 (3)	−1.35	−0.22	−0.32 (3)	−1.31	−0.21	−1.33	−0.23
N	0.08 (7)	−1.06	−0.03	−0.01 (8)	−1.08	−0.03	−0.92	0.01
C	−0.14 (7)	−0.13	−0.09	−0.18 (9)	−0.29	−0.08	−0.23	−0.06
H1	0.04 (3)	0.07	0.08	0.09 (4)	0.07	0.09	0.07	0.07
H2	0.08 (3)	0.09	0.09	0.07 (4)	0.04	0.08	0.03	0.06
H3	0.21 (3)	0.48	0.20	0.26 (4)	0.49	0.20	0.42	0.18
H4	0.20 (3)	0.50	0.22	0.22 (4)	0.51	0.22	0.46	0.18
H5	0.23 (3)	0.50	0.21	0.24 (4)	0.51	0.22	0.43	0.18
H6	0.31 (3)	0.58	0.21	0.28 (5)	0.60	0.24	0.56	0.16
Group								
PO_3H	−0.67	−0.44	−0.68	−0.73	−0.17	−0.71	−0.26	−0.61
CH_2	−0.02	0.03	0.08	−0.02	−0.15	0.09	−0.13	0.07
NH_3	0.72	0.42	0.60	0.71	0.34	0.61	0.39	0.55

Table 3
Essential bond topological parameters together with Wiberg bond indices.

	ρ_c (e Å^{-3})			$\nabla^2\rho_c$ (e Å^{-5})		ε (ellipticity)		Wiberg bond indices
Refinement	(I)	(II)	TZ2P	(I)	(II)	(I)	(II)	TZ2P
P—O1	1.81 (3)	1.670 (9)	1.57	3.5 (2)	22.45 (4)	0.05	0.11	1.23
P—O2	1.72 (2)	1.584 (8)	1.51	0.5 (2)	19.08 (3)	0.06	0.07	1.18
P—O3	1.48 (2)	1.340 (6)	1.25	−2.3 (1)	14.34 (3)	0.04	0.13	0.70
P—C	1.24 (2)	1.167 (7)	1.01	−7.53 (4)	−5.40 (2)	0.02	0.06	0.70
O3—H6	2.16 (5)	2.26 (7)	2.34	−40.2 (4)	−43.7 (6)	0.06	0.01	0.73
N—C	1.66 (3)	1.66 (2)	1.48	−8.01 (6)	−8.54 (4)	0.06	0.07	0.90
N—H3	2.18 (7)	2.15 (7)	2.25	−29.8 (4)	−31.3 (5)	0.01	0.02	0.79
N—H4	2.24 (6)	2.24 (7)	2.18	−32.4 (4)	−33.5 (4)	0.04	0.05	0.74
N—H5	2.20 (7)	2.21 (7)	2.25	−33.9 (4)	−35.2 (5)	0.03	0.02	0.78
C—H1	1.92 (6)	1.93 (6)	1.66	−19.9 (2)	−20.3 (2)	0.05	0.03	0.91
C—H2	1.89 (6)	1.93 (7)	1.66	−19.5 (2)	−20.4 (3)	0.06	0.06	0.91
Hydrogen bond								
O1···H5^{i}	0.25 (3)	0.25 (3)	–	1.53 (5)	1.45 (6)	0.13	0.10	–
O2···H3^{ii}	0.25 (3)	0.26 (3)	–	2.20 (5)	1.98 (5)	0.04	0.11	–
O2···H6^{iii}	0.43 (3)	0.40 (3)	–	1.23 (7)	1.65 (8)	0.14	0.05	–

Symmetry codes: (i) $-x, \frac{3}{2}-y, \frac{1}{2}+z$; (ii) $-\frac{1}{2}+x, y, \frac{1}{2}-z$; (iii) $-\frac{1}{2}-x, -\frac{1}{2}+y, z$.

density in the critical point of the respective bond) and $\nabla^2\rho_c$ (Laplacian of the former) reveals that both refinements have yielded similar values for the bonds which do not include the P atom. Also the differences of ρ_c (e Å^{-3}) for the P—O and P—C bonds are moderate. In the general refinement (II) has given smaller values of ρ_c for all bonds and these values are closer to those derived from the DFT calculations (Table 3). The most noticeable difference between the two refinements lies in the values of Laplacian for the P—O bonds, which are an order of magnitude greater for refinement (II). Apart from that the value for the P—O3 bond assumes a slightly negative value in the case of refinement (I). However, some common features may be observed:

(i) as far as the P—O bonds are concerned the values of ρ_c and $\nabla^2\rho_c$ are higher when the O atom does not bind a H atom; the Laplacian is positive for P—O1 and P—O2 – this indicates a significant fraction of ionic character in these bonds;

(ii) in the case of the P—C bond ρ_c is smaller than those for P—O and the Laplacian is slightly negative.

Apart from that a positive correlation between ρ_c and Wiberg bond order may be noticed for the P—O bonds. These data may be compared with the literature data. In HPPM ρ_c and $\nabla^2\rho_c$ (e Å^{-5}) for the P—O bonds are in the range 1.49–1.50 and 27.10–28.17, whereas for P—OH ρ_c is 1.28 and $\nabla^2\rho_c$ – 17.90. For P—C these values are 1.09 and −3.90. Generally these parameters are more similar to our refinement (II). The values for the N—C(—P), N—H and O—H bonds are similar to ours. In ammonium dihydrogen phosphate the following values were obtained: P—O: ρ_c = 1.68, $\nabla^2\rho_c$ = 16.2; P—OH: ρ_c = 1.46, $\nabla^2\rho_c$ = 6.93; in L-arginine dihydrogen phosphate: P—O: ρ_c = 1.62, $\nabla^2\rho_c$ = 16.06; P—OH: ρ_c = 1.46, $\nabla^2\rho_c$ = 7.44; in $AlPO_4$-15 for the P—O bonds ρ_c = 1.55–1.67, $\nabla^2\rho_c$ = 3.4–8.4 (remarkably low). To find to what extent the ρ_c values for the P—O and P—C bonds result from the simple overlapping of spherical densities of isolated atoms, which vary with the interatomic distances, and what part of these quantities is the excess resulting from donation of the electron density to the bonds (Aubert *et al.*, 2003), we have calculated the differences between the values of the charge density from refinement (II) and calculated critical points for the promolecule in refinement (II). The differences {hereinafter Δ[(II),iam]ρ_c} were for: P—O1 0.378 (10), P—O2 0.333 (8), P—O3 193 (7) and P—C 0.282 (8) e Å^{-3}. The ellipticities of the P—O bonds gained from the two refinements are in moderate agreement; this is the result of different eigenvalues of the respective Hessians, which are in turn a consequence of the different modeling of the electron density around phosphorus. However, it may be noticed that the values reported in the literature also vary to some extent. In HPPM they are close to 0 (more precisely in the range 0.03–0.06) for both P—O and P—O(H) bonds, while for L-arginine dihydrogen phosphate or ammonium dihydrogen phosphate they are

Table 4
The strongest delocalization effects in the aminomethylphosphonic acid molecule.

n_d, n_a: occupation numbers of donor and acceptor orbitals; $E(2)$: stabilization energy (kJ mol^{-1}), ΔE: energy difference between acceptor and donor (a.u.); F_{ij}: cross element of the Fock matrix (a.u.).

Donor	Acceptor	n_d	n_a	$E(2)$	ΔE	F_{ij}
O1(lp)	σ^*(P—O2)	1.81	0.13	49.15	0.52	0.071
O1(lp)	σ^*(P—O3)	1.81	0.23	68.08	0.42	0.075
O1(lp')	σ^*(P—C)	1.79	0.22	78.08	0.37	0.075
O2(lp)	σ^*(P—O1)	1.80	0.14	44.25	0.53	0.068
O2(lp)	σ^*(P—C)	1.80	0.22	65.69	0.39	0.070
O2(lp')	σ^*(P—O3)	1.82	0.23	81.27	0.43	0.083
O3(lp)	σ^*(P—O1)	1.92	0.14	26.59	0.64	0.058
O3(lp)	σ^*(P—C)	1.92	0.22	34.37	0.49	0.059

between 0.06 and 0.20, the higher values being for the P—O(H) bonds.

Refinement (I) was designed to adhere to the pattern applied previously (with the exception of refining the κ' parameters which we were unable to perform) for the majority of systems containing P atoms. The other refinement (II) was based on the following. In all the non-H atoms (including phosphorus, as it results from the discussion in §1) only *ns* and *np* orbitals are filled and take part in forming the bonds. The electron density based on these orbitals may be in principle expanded up to quadrupolar terms. The octupoles were then added to allow for polarization terms (resulting from products of *p* and *d* orbitals). For reasons explained in §2 the deformation densities of the H atoms were expanded up to quadrupolar terms. The two models presented have given results of similar quality as far as such global quality descriptors as residual differential Fourier synthesis or the *R* indices are taken into account. Refinement (I) yielded a smoother distribution in what may be seen in higher ρ_c and lower $\nabla^2\rho_c$ values. The experimental charges of all atoms, except P, are within the previously reported range; the P multipolar charge found in refinement (II) was exceptionally small compared with the values quoted in the literature. On the other hand, the Bader charges of P and C derived from model (II) are in better agreement with the theoretical values. The values of ρ_c from both refinements are similar to those reported for other P systems, whereas $\nabla^2\rho_c$ values from refinement (II) better match the values of charge density Laplacian found for other phosphorus compounds. Generally it seems that the refinement of κ' parameters for P was more essential than the inclusion of hexadecapole parameters.

In order to elucidate the character of P—O and P—C bonding interactions we performed the natural bond orbitals (NBO; Glendening *et al.*, 2001) and Natural Resonance Theory (NRT) analysis (Glendening & Weihold, 1998) The phosphonates belong to the class of hypervalent compounds, *i.e.* the compounds that seem to break the octet rule and that cannot be described well by single Lewis formulae. Hypervalency has been the subject of extensive investigations and it is beyond the scope of this paper to examine it in detail; more thorough discussion of this phenomenon in the case of phosphorus may be found in the literature (Magnusson, 1990; Gilheany, 1994; Denehy *et al.*, 2007). As has been pointed out in §1 participation of the *d* orbitals of phosphorus in the P—O and P—C bonds has been ruled out on the basis of computational evidence and the results of our calculations do not support the opposite view either. Therefore, we shall limit our discussion to the interplay of the *s* and *p* orbitals only. The *d* orbitals have proved to be polarization functions which slightly modify the *s*/*p* orbital framework. Whenever their role is more than negligible this will be marked. Below we would like to present our results. The Wiberg bond indices in the natural atomic orbitals basis are presented in Table 3. It may be noticed that the indices for the P—O(unprotonated) bond are much larger (*ca* 1.2) than for the P—O(H) and P—C ones (*ca* 0.7). In the NBO approach there are only single bonding orbitals within the aminomethylphosphonic acid molecule. Their calculated compositions are the following:

(i) P—O1: 0.518P($sp^{2.22}$) + 0.855O1($sp^{2.30}$),
(ii) P—O2: 0.510P($sp^{2.38}$) + 0.860O2($sp^{2.10}$),
(iii) P—O3: 0.464P($sp^{3.62}d^{0.12}$) + 0.886O3($sp^{2.30}$),
(iv) P—C: 0.555P($sp^{4.06}d^{0.12}$) + 0.832C($sp^{2.76}$).

Apart from that there are three lone pairs located on each of the unprotonated O1 and O2 atoms, as well as two pairs on O3. They have the following hybridizations: O1: $sp^{0.44}$ and two *p* pairs, O2: $sp^{0.48}$ and two *p* pairs, O3: $sp^{1.09}$ and *p*. These results may be summarized as follows. The P atom utilizes sp^2 hybrids to form bonds with unprotonated O atoms, whereas sp^4 combinations are involved in bonds with the protonated O3 and C. The O atoms use sp^2 hybrids to bond to phosphorus. All the bonds are highly polarized: P—O(unprotonated) *ca* 50%, P—O3 60% and P—C 40%. In the framework of the NBO method the delocalization within the molecule may be traced indirectly. This effect should be considered if there are high energies of stabilization due to delocalization interactions between occupied lone pairs or bonding orbitals, and empty Rydberg or antibonding orbitals, accompanied by depleted occupation of the bonding orbitals (which should be 2 in the ideal case) and partial population of the initially empty Rydberg and/or antibonding ones. The interaction energy is usually calculated in the second order of the perturbation theory and is expressed as $E(2) = n_j F_{ij}/\Delta E_{ij}$, where F_{ij} is the cross element of the Fock matrix between the acceptor and donor orbitals, ΔE_{ij} is the energy difference between the two orbitals, and n_j is the occupation of the donor (Denehy *et al.*, 2007). In our case these effects concentrate within C—PO_3 and the strongest interactions are shown in Table 4 apart from that smaller values of $E(2)$ (13.44–15.78 kJ mol^{-1}) have been calculated for σ(C—P) $\rightarrow$ σ^*(P—O1,2,3) charge transfers. These energies are slightly smaller than those calculated for methyl phosphate $CH_3OPO_3^{2-}$ (Denehy *et al.*, 2007), where they are [for terminal oxygen lone pairs as the donors and σ^*(P—$O_{terminal}$) as the acceptors] in the range 61.55–79.97 kJ mol^{-1}. The lone pairs of the O atoms that undergo delocalization are exclusively of *p* character. Inspection of Table 4 reveals that the most active are the pairs of unprotonated O1 and O2 atoms, whereas the O3 pair interacts less efficiently. The reason for this lies in the greater energy difference ΔE between the donor and acceptor orbitals in the

case of O3, which renders mixing of the respective orbitals less efficient. The greater value of ΔE, in turn, is brought about by greater stabilization of the *p* lone pair of O3 involved in the delocalization – its energy is −0.291 a.u. (atomic units) – than the energies of the *p* lone pairs of O1 and O2 – their energies being in the range −0.187 to −0.171 a.u., depending on the pair. The stabilization may be interpreted as being caused by the neighborhood of the H6 atom, attached to O3. Generally, the delocalization described above results in donation of part of the electron density from lone pairs of O1 and O2 to antibonding orbitals σ^*(P—C) and σ^*(P—O3), which is reflected in the reduced values of calculated Wiberg indices of these bonds. To illustrate these mechanisms an example of overlapping of a lone pair of O2 with the antibonding obital σ^*(C—P) is presented in Fig. 3.

To get an overall and more intuitive insight into the character of bonding interactions within the phosphonate group we have calculated the possible resonance Lewis structures, which are presented in Fig. 4. As the calculations performed with the two bases TZ2P and ET gave somewhat different results, both results will be presented here. Structure (I) may be regarded as the basic one because of the most equalized distribution of the charge density. In this form the positively charged P atom is bonded through four single bonds to two negatively charged O anions, the OH group and the C atom. Its share in the resonance hybrid is 15% in the case of TZ2P calculations and 10% for the ET model. Structures (II), (III) and (V) represent various cases of hyperconjugation among the O atoms. Their total weight is 37% for TZ2P and 40% for ET. Structure (V) has emerged from the TZ2P calculations only; in ET it has been absorbed [together with part of structure (I)] in structure (III). It is noteworthy that the double [or triple in the case of form (V)] bonds are formed only with the unprotonated O atoms. The practical absence of forms with a double bond between P and O3 is in accordance with the lower energies of the O3 lone pairs, as discussed above. The overall effect of the described hyperconjugation is that the bond orders of P—O1 and P—O2 increase, with a concomitant decrease of the P—O3 bond order, which is manifested in different Wiberg indices of bonds P—O1 and P—O2 on one side, and P—O3 on the other. This mechanism reflects in the experimental charge density distribution by greater accumulation of the negative charge in O1 and O2

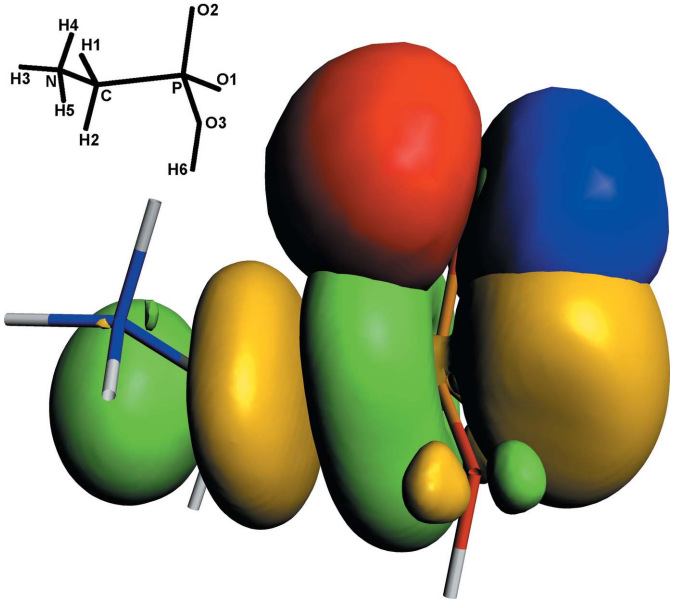

Figure 3
Overlapping between a lone pair of O2 (upper, red–blue) with the antibonding orbital σ^*(P—C) (lower, yellow–green), giving rise to a partial charge transfer to the latter. The molecule orientation is shown in the insert.

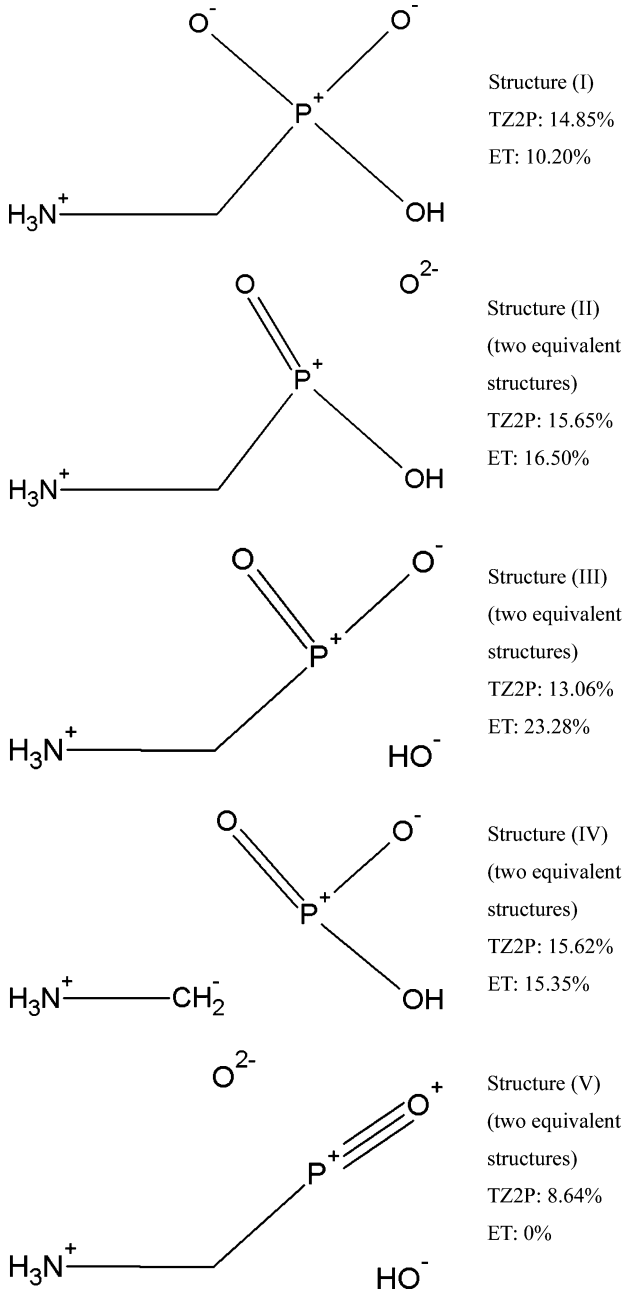

Figure 4
Calculated leading resonance Lewis structures and their resonance weights for aminomethylphosphonic acid. For simplicity the unprotonated O1 and O2 atoms are treated as equivalent.

compared with O3, and greater values of Δ[(II),iam]ρ_c for P—O1 and P—O2 in comparison with P—O3. Form (IV) represents hyperconjugation between C and the unprotonated O atoms. Its contribution brings about reduction of the average bond order of P—C and strengthening of the bonds P—O1 and P—O2. In the experimental map this is reflected by a low ρ_c(P—C) value, 1.24 (2) e Å^{-3} for refinement (I) and 1.167 (7) e Å^{-3} for refinement (II). The other result of the presence of this form is the transfer of a certain amount of negative charge onto C, which indeed may be observed for the charges calculated from the experimental data.

It must be said, however, that the above considerations concern an isolated molecule; the introduction of hydrogen bonds may modify to some extent the details of the interactions. Unfortunately, owing to problems with the convergence we could not calculate the wavefunctions for a cluster of aminomethylphosphonate molecules. The hydrogen bonds give rise to polarization of the electron clouds around the O atoms, which may be best viewed on deformation density maps (Fig. 5). The basic topological parameters of the hydrogen bonds (ρ_c, $\nabla^2\rho_c$ and ε; see Table 3) are in good agreement with the analogous parameters found in other crystals (Espinosa *et al.*, 1996, 1999; Slouf *et al.*, 2002). These parameters could not be calculated for a long O1···H4^{iv} bond (O1···H4^{iv} 2.03 Å; for the other three hydrogen bonds listed in Table 3 the O···H distances are 1.60–1.78 Å).

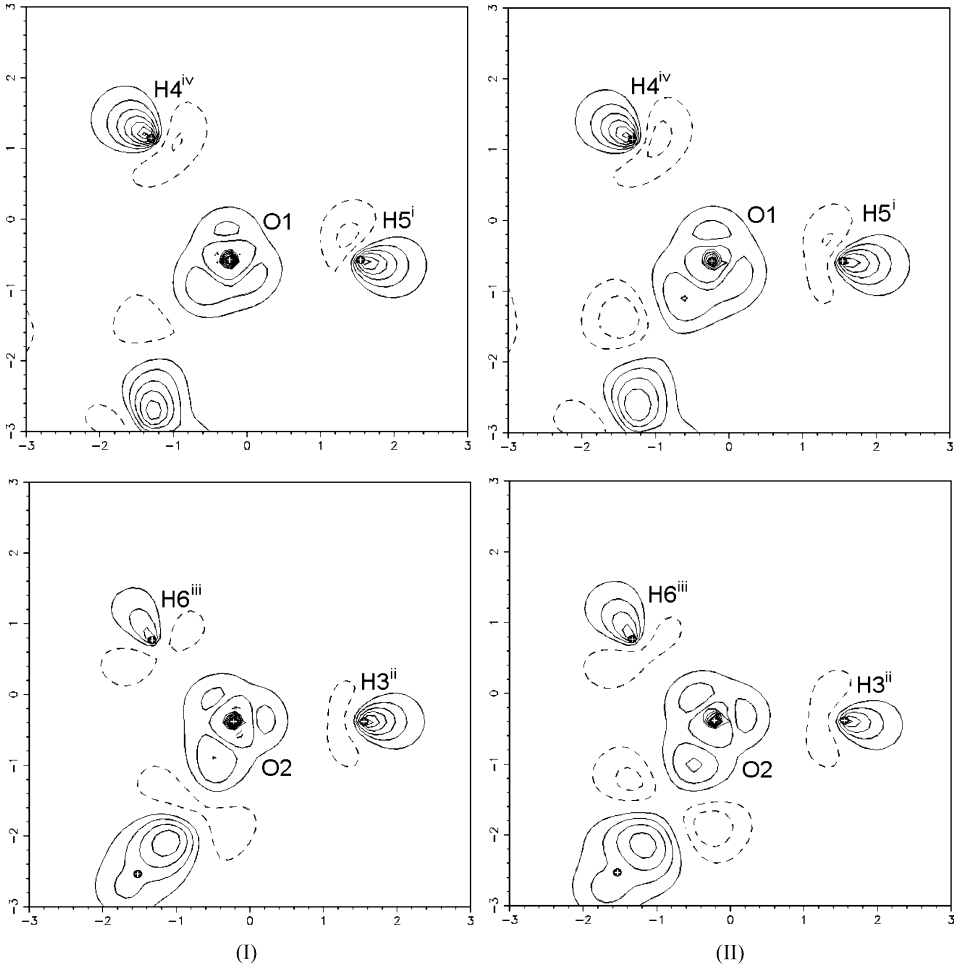

Figure 5
Deformation density maps from multipole refinements (I) and (II). The contour intervals are drawn at 0.1 e Å^{-3}. The positive contours are solid, the negative contours dashed and the zero contours have been omitted. The atoms shown define the section plane; the scale is in Å.

4. Conclusions

The experimental charge density distribution of aminomethylphosphonic acid has been determined and discussed with respect to the results of theoretical DFT calculations.

The phosphonate group may be perceived in the first approximation as composed of a P^+ cation connected to a C atom, two O^- anions and an OH group with highly polarized covalent bonds, in a manner somewhat analogous to the bonding scheme proposed for quaternary ammonium or phosphonium cations (N^+R_4 or P^+R_4). This basic bonding pattern is modified by massive hyperconjugation effects which lead to weakening of the P—C and P—O(H) bonds along with strengthening and polarization of the P—O bonds. This may be observed as relative changes of ρ_c of the respective bonds in the experimental charge density maps. The P—O(H) and P—C bonds are destabilized by donation of part of the electron density from lone pairs of unprotonated O atoms to relevant antibonding σ^*(P—O) and σ^*(P—C) orbitals. This, in turn, leads to the growth of experimental and theoretical negative Bader and Hirshfeld charges of unprotonated compared with protonated O atoms. The increased negative charge of the C atom is another result of hyperconjugation. It has been demonstrated that the charge density around the P atom may be effectively modelled with multipolar expansion up to octupoles, which is consistent with the assumption of the non-involvement of phosphorus *d* orbitals in the P—O and P—C bonds.

The authors thank Professor T. Lis for the data collection and valuable discussion. The ADF calculations have been carried out at the Wrocław Centre for Networking and Supercomputing (http://www.wcss.wroc.pl), grant No. 58.

References

Allen, F. H., Kennard, O., Watson, D. G., Brammer, L., Orpen, A. G.

& Taylor, R. (1987). *J. Chem. Soc. Perkin Trans. 2*, pp. S1–S19.
Aubert, E., Porcher, F., Souhassou, M. & Lecomte, C. (2003). *Acta Cryst.* B**59**, 687–700.
Bader, R. F. W. (1990). *Atoms in Molecules. a Quantum Theory.* Oxford University Press.
Baerends, E. J. *et al.* (2008). *ADF*2008.01, SCM. Theoretical Chemistry, Vrije Universiteit, Amsterdam, The Netherlands, http://www.scm.com.
Blessing, R. H. (1987). *Crystallogr. Rev.* **1**, 3–58.
Brandenburg, K. & Putz, H. (2005). *DIAMOND*, Version 3.0a. Crystal Impact GbR, Bonn, Germany.
Clementi, E. & Roetti, C. (1974). *At. Data Nucl. Data Tables*, **14**, 177–478.
Darriet, M., Darriet, J., Cassaigne, A. & Neuzil, E. (1975). *Acta Cryst.* B**31**, 469–471.
Denehy, E., White, J. M. & Williams, S. J. (2007). *Inorg. Chem.* **46**, 8871–8886.
Espinosa, E., Lecomte, C., Molins, E., Veintemillas, S., Cousson, A. & Paulus, W. (1996). *Acta Cryst.* B**52**, 519–534.
Espinosa, E., Souhassou, M., Lachekar, H. & Lecomte, C. (1999). *Acta Cryst.* B**55**, 563–572.
Finlay, I. G., Mason, M. D. & Shelley, M. (2005). *Lancet Oncol.* **6**, 392–400.
Gasiglia, H. T. & Okada, H. (1995). *J. Radioanal. Nucl. Chem. Lett.* **199**, 295–304.
Gilheany, D. G. (1994). *Chem. Rev.* **94**, 1339–1374.
Glendening, E. D., Badenhoop, J. K., Reed, A. E., Carpenter, J. E., Bohmann, J. A., Morales, C. M. & Weinhold, F. (2001). *NBO* 5.0. Theoretical Chemistry Institute, University of Wisconsin, Madison, USA.
Glendening, E. D. & Weihold, F. (1998). *J. Comput. Chem.* **19**, 593–609.
Hansen, N. K. & Coppens, P. (1978). *Acta Cryst.* A**34**, 909–921.
Hirshfeld, F. L. (1976). *Acta Cryst.* A**32**, 239–244.
Hirshfeld, F. L. (1977). *Theor. Chim. Acta*, **44**, 129–138.
Hudson, R. F. (1964). *Pure Appl. Chem.* **9**, 371–386.
Ichikawa, M., Gustafsson, T. & Olovsson, I. (1998). *Acta Cryst.* B**54**, 29–34.
Janicki, R. & Mondry, A. (2008). *Polyhedron*, **27**, 1942–1946.
Lyssenko, K. A., Grintselev-Knyazev, G. V. & Antipin, M. Yu. (2002). *Mendeleev Commun.* pp. 128–130.
Magnusson, E. (1990). *J. Am. Chem. Soc.* **112**, 7940–7951.
Mao, J.-G. (2007). *Coord. Chem. Rev.* **251**, 1493–1520.
Mitchell, K. A. R. (1969). *Chem. Rev.* **69**, 157–178.
Mondry, A. & Janicki, R. (2006). *Dalton Trans.* pp. 4702–4710.
Murphy, P. J. (2004). *Organophosphorus Reagents.* Oxford University Press.
Oxford Diffraction Ltd (2010). *CrysAlis* CCD, Version 1.171.33. Oxford Diffraction Ltd, Abingdon, Oxfordshire, England.
Parker, D. (2004). *Chem. Soc. Rev.* **33**, 156–165.
Pérès, N., Boukhris, A., Souhassou, M., Gavoille, G. & Lecomte, C. (1999). *Acta Cryst.* A**55**, 1038–1048.
Rodrigues, B. L., Tellgren, R. & Fernandes, N. G. (2001). *Acta Cryst.* B**57**, 353–358.
Savigniac, P. & Iorga, B. (2003). *Modern Phosphonate Chemistry*. Boca Raton, FL, USA: CRC Press LLC.
Schomaker, V. & Stevenson, D. P. (1941). *J. Am. Chem. Soc.* **63**, 37–40.
Schwartz, A. W. (2006). *Philos. Trans. R. Soc. London Ser. B*, **361**, 1743–1749.
Sheldrick, G. M. (2008). *Acta Cryst.* A**64**, 112–122.
Slouf, M., Holy, A., Petříček, V. & Cisarova, I. (2002). *Acta Cryst.* B**58**, 519–529.
Souhassou, M., Espinosa, E., Lecomte, C. & Blessing, R. H. (1995). *Acta Cryst.* B**51**, 661–668.
Volkov, A. & Coppens, P. (2001). *Acta Cryst.* A**57**, 395–405.
Volkov, A., Macchi, P., Farrugia, L. J., Gatti, C., Mallinson, P., Richter, T. & Koritsánszky, T. (2006). *XD*2006. University at Buffalo, NY; University of Milano, Italy; University of Glasgow, UK; CNRISTM, Milano, Italy; Middle Tennessee State University, TN, USA.
Westheimer, F. H. (1987). *Science*, **235**, 1173–1178.
Wiberg, K. B. (1968). *Tetrahedron*, **24**, 1083–1096.
Winter, P. M., Seshan, V., Makos, J. D., Sherry, A. D., Malloy, C. R. & Bansal, N. (1998). *J. Appl. Physiol.* **85**, 1806–1812.